Ground-state phase diagrams of the generalized Falicov-Kimball model with Hund coupling

Romuald Lemański and Jakub Wrzodak
Institute of Low Temperature and Structure Research, Polish Academy of Sciences, 50-422 Wrocław, Poland
(Received 19 December 2007; revised manuscript received 10 July 2008; published 14 August 2008)

Charge and spin orderings are studied on the simplest one-dimensional (1D) and the two-dimensional (2D) square lattices within the generalized Falicov-Kimball model with Hund coupling between localized and itinerant electrons. Using the restricted phase diagram method (RPDM), a number of simple rules of formation of various sorts of ground-state phases have been detected. In particular, relationships between density of current carriers (electrons or holes) and type of charge and magnetic arrangement have been determined. In two dimensions in the mixed-valence regime, only axial stripes (vertical or horizontal) have been found for intermediate values of the coupling constants. They are composed of ferromagnetic or antiferromagnetic chains interchanged with nonmagnetic ones. For band fillings close to the half filling, stripe phases oriented along one of the main diagonal direction are formed. The results suggest the possibility of tuning modulations of charge and magnetic superstructures with a change in doping.

DOI: 10.1103/PhysRevB.78.085118 PACS number(s): 71.10.Fd, 71.28.+d

I. INTRODUCTION

Charge and magnetic superstructures observed in many transition-metal oxides, such as, e.g., in $R_{2-x}Sr_xNiO_4$, where R=La,Nd,[1] have stimulated an intensive search for an explanation of the origins of the phenomenon and its impact on the physical properties of the systems. The subject has been analyzed primarily in the framework of various versions of the Hubbard or t-J model.[2–9]

An alternative approach based on the spinless Falicov-Kimball model (FKM) was proposed in Ref. 10. Within the space restricted to a large number of the simplest trial configurations, the ground-state diagrams have been found exactly showing how the chessboard phase evolves to phase separation with a change in doping. It appeared that quite large areas of the diagrams are occupied by stripe phases oriented either along one of the main crystallographic axes (*axial stripes*) or along one of the main diagonals (*diagonal stripes*). These findings were confirmed by rigorous studies.[11]

The spinless FKM is simple enough to obtain controllable results for all values of the coupling constant. However, the model can deal only with charge-ordered phases and it neglects magnetic properties. To overcome this shortcoming, a generalized version of the spin-one-half FKM with a spin-dependent local term representing Hund's first rule was proposed in Ref. 12. An important role of the Hund coupling in explaining the magnetic properties of correlated electron systems was raised, e.g., in Refs. 13–15 and specifically in applying to the FKM in Ref. 16. In fact, the model we deal with is very similar to the ferromagnetic Kondo lattice model, which was also considered in the context of charge and magnetic superstructures in correlated electron systems.[14,17]

Here we assume that the simplest Ising-type anisotropy of the Hund coupling is what enables us to examine the model rigorously. The anisotropy is relevant in systems where spin-flip processes have a minor meaning and stable magnetically ordered phases occur (for more arguments, see Ref. 12).

The extended model is still oversimplified to describe all details of real materials. However, since it comprises only basic interactions, which are present in all materials, where both localized and itinerant electrons are relevant, we expect that its characteristics emerging from our calculations are quite universal. Our expectations are justified by the fact that phases similar to those we detected were also found by other authors who studied different models and used quite different methods, as it was reported, e.g., in Ref. 6 for a version of the Hubbard model and in Refs. 14 and 17 for the ferromagnetic Kondo (or Hund) lattice model.

In Ref. 12 only some basic properties of the model in two dimensions were examined. Farkašovský and Cencariková[18] studied the model by means of small-cluster exact-diagonalization calculations and an efficient numerical method for large clusters containing up to 64 lattice sites. They constructed phase diagrams, where they found a number of various types of charge and spin distributions and observed a gradual reduction in the stability region of the nonpolarized (NP) phase in favor of the fully polarized (FP) and partially polarized (PP) phases with an increase in the Hund coupling and with an increase in the number of localized particles. The studies are interesting, as they enabled examination of the model in a complementary way. However the obtained results are too general for making predictions on details of charge and spin ordering for a given set of model parameters. Moreover, there are some strange irregularities in their diagrams. For example, for small Hund couplings or for small densities of both localized and itinerant particles, one can find the FP phase at some isolated positions, surrounded by NP phases. In addition a lack of PP phases in a wide region of the diagram close to the chessboard AF phase, especially for small J, seems to be an artifact resultant of taking into consideration only clusters with even numbers of sites.

A need for a clarification of this picture pushes us to examine the model more carefully. In our previous work we considered only the two-dimensional (2D) case and we used a too small configurational space to detect many regularities. We noticed merely a few general tendencies for the formation of charge- and/or spin-ordered phases.[12] Here we expand upon our preceding work to both one-dimensional (1D) and 2D systems and provide a thorough analysis of the ground-

state phase diagrams using a much larger set of admissible configurations. It allows us to notice some simple rules of formation of periodic phases (as well as their mixtures) not noticed in previous studies.

The model Hamiltonian is

$$H = t\sum_{\langle i,j\rangle}\sum_{\sigma=\uparrow,\downarrow} d^{\dagger}_{i,\sigma}d_{j,\sigma} + U\sum_{i}\sum_{\sigma,\eta=\uparrow,\downarrow} n^{d}_{i,\sigma}n^{f}_{i,\eta} - J\sum_{i}(n^{d}_{i,\uparrow}-n^{d}_{i,\downarrow})(n^{f}_{i,\uparrow}-n^{f}_{i,\downarrow}), \quad (1)$$

where $\langle i,j\rangle$ denotes the nearest-neighbor lattice sites i and j, σ and η are spin indices, $d_{i,\sigma}$ ($d^{\dagger}_{i,\sigma}$) is an annihilation (creation) operator, and $n^{d}_{i,\sigma}$ ($n^{f}_{i,\eta}$) is an occupation number of itinerant (localized) electrons. The on-site interaction between localized and itinerant electrons is represented by two coupling constants: U, which is spin-independent Coulomb type, and J, which is spin dependent and reflects the Hund's rule force. The hopping amplitude t is set equal to 1, so we measure all energies in units of t.

Double occupancy of the localized electrons is forbidden, implying that the on-site Coulomb repulsion U_{ff} between two f electrons is infinite. Consequently, at a given site the f-electron occupancy is assumed to be $n_f=n_{f,\uparrow}+n_{f,\downarrow}\leq 1$ and the d-electron occupancy to be $n_d=n_{d,\uparrow}+n_{d,\downarrow}\leq 2$. Thus there are three states per site allowed for the f electrons ($n_f=0$; $n_{f,\uparrow}=1$ and $n_{f,\downarrow}=0$; $n_{f,\uparrow}=0$ and $n_{f,\downarrow}=1$) and four states per site allowed for the d electrons ($n_d=0$; $n_{d,\uparrow}=1$ and $n_{d,\downarrow}=0$; $n_{d,\uparrow}=0$ and $n_{d,\downarrow}=1$; $n_d=2$).

All single-ion interactions included in Eq. (1) preserve states of localized electrons; i.e., the itinerant electrons traveling through the lattice change neither the occupation numbers nor the spins of the localized ones. Then $[H,f^{+}_{i\eta}f_{i\eta}]=0$ for all i and η, so the local occupation number is conserved.

The localized electrons play the role of an external charge- and spin-dependent potential for the itinerant electrons. This external potential is "adjusted" by annealing, so the total energy of the system attains its minimum. In other words, there is a feedback between the subsystems of localized and itinerant electrons. This is the feedback that is responsible for the long-period-ordered arrangements of the localized electrons and consequently for the formation of various charge and/or spin distributions at low temperatures.

In Sec. II we briefly describe our calculation scheme. Then, in Sec. III we present two kinds of phase diagrams referring to pure magnets (Sec. III A) and diluted magnets (Sec. III B). Section IV contains the summary and discussion.

II. RESTRICTED PHASE DIAGRAM METHOD

We used the restricted phase diagram method (RPDM) first in our studies of the spinless 1D FKM in Ref. 19 and then also in Refs. 10, 12, and 20. Within the method, calculations are performed for infinite systems but with a restriction to periodic phases, with periods not exceeding a certain value, and their mixtures. Then, we can investigate both periodic phases and phase separation and segregation.

We emphasize that the RPDM is by no means a mean-field approach and the calculations refer to infinite systems, not to finite clusters. So we do not need to deal with neither boundary nor finite-size effects. The energies (per site) of all phases we consider here are evaluated with a very high and controllable accuracy. For small period phases with no more than four lattice sites in a unit cell, energy bands are given by analytical expressions,[21] and the precision is limited merely by the selection of a grid in the k space. For large period phases some very small errors, resulting from numerical diagonalization of matrices of size of the number of lattice sites in a unit cell, may additionally enter. The details of the current work are as follows.

We performed calculations in one dimension and two dimensions (the square lattice) for $U=1$, 2, 4, 6, and 8 and J changing from $0.2U$ up to $0.75U$ and within the configurational space restricted to all periodic phases with unit cells containing up to 12 lattice sites for pure magnets and up to 8 for diluted magnets. To assure the stability of the phases appearing on the diagrams, we constructed *the grand canonical phase diagrams* first (see Refs. 19 and 20 for a more detailed discussion of the stability issue) on the plane of the chemical potentials. Then we transformed the diagrams into the canonical phase diagrams on the plane of the densities of localized (ρ_f) and itinerant (ρ_d) electrons. By applying this procedure, one automatically includes all mixtures of the phases. The resulting phase diagrams are quite sensitive to the values of the interaction parameters U and J. In general, they have a rich structure composed of various families of phases.

In order to calculate the Gibbs thermodynamic potential, we first determined the electronic band structure for the itinerant electrons for each candidate periodic phase. We employed a sufficiently tiny grid in the Brillouin zone (up to $N_c=100$ momentum points in one dimension and up to $N_c=80\times 80$ in two dimensions for each band structure). This required us to diagonalize up to 12×12 matrices in the pure magnet case and up to 8×8 matrices in the diluted magnet case at each discrete momentum point in the Brillouin zone. This results in at most 12 and 8 different energy bands in the pure and diluted magnet cases, respectively. Hence, our calculations can be viewed as finite size but very large cluster calculations with cluster sizes ranging in one dimension from $N=100$ up to $N=100\times 12$ in the pure magnet case and from $N=100$ up to $N=100\times 8$ in the diluted magnet case. On the other hand, in two dimensions the cluster sizes range from $N=80\times 80$ up to $N=80\times 80\times 12$ in the pure magnet case and from $N=80\times 80$ up to $N=80\times 80\times 8$ in the diluted magnet case, depending on the number of sites in the unit cell. ($N=N_cC$, where N_c is equal to the number of unit cells and C denotes the number of lattice sites in a unit cell for a given configuration of localized electrons.)

We performed all the calculations separately for spin-up and -down itinerant electrons. The eigenvalues of the band structure are summed up to determine the ground-state energy for each density of the electrons. Then, the Gibbs thermodynamical potential for a given configuration $\{w_f\}$ is calculated for all possible values of the chemical potentials μ_d and μ_f of the conduction and localized electrons, respectively, through the formula

$$G_{\{w_f\}} = \frac{1}{N} \sum_{\varepsilon_\uparrow, \varepsilon_\downarrow < \mu_d} [\varepsilon_\uparrow(\{w_f\}) + \varepsilon_\downarrow(\{w_f\})] - \mu_d(\rho_{d\uparrow} + \rho_{d\downarrow}) - \mu_f(\rho_{f\uparrow} + \rho_{f\downarrow}), \quad (2)$$

where the symbol $\varepsilon_\uparrow(\{w_f\})$ $[\varepsilon_\downarrow(\{w_f\})]$ denotes the energy eigenvalues of a band structure attributed to spin-up (-down) itinerant electrons for a given configuration $\{w_f\}$ of localized electrons.

It appears that only a small part of the initial candidate phases can be found in the ground-state phase diagram. The actual number depends on U, J, and C but the rate drops drastically with an increase in C. We find that for the values of the parameters we considered, it is less than 10% in the 1D case and less than 2% in the 2D case.

III. PHASE DIAGRAMS

In this paper we present two types of the ground-state phase diagrams. The first type (*pure magnets*) demonstrates only magnetic order, as it corresponds to the case $\rho_f=1$ (each site is occupied by exactly one *f electron*) on the plane (J,ρ_d). The second type (*diluted magnets*) demonstrates both a magnetic and a charge order on the plane (ρ_d,ρ_f) for fixed values of J and U. The diagrams show the ground-state configurations of the f electrons in both one dimension and two dimensions for representative values of the model parameters. For a pure magnet we selected $U=4$, $0.2 \leq J \leq 3.0$ in one dimension and $U=6$, $0.2 \leq J \leq 3.0$ in two dimensions. For the diluted magnet $U=2$, $J=0.5$ in one dimension and $U=4$, $J=0.5$ in two dimensions.

A. Pure magnets

In the pure magnetic diagrams the ferromagnetic (F) phase is stable for ρ_d close to 0 or 2 and the region of the stability increases with J, whereas along the line $\rho_d=1$ (the half filling) the simplest AF phase is stable. Now, the most interesting story concerns a way of transforming between the two extreme phases with a change in ρ_d.

Obviously, the process depends on J, but it is the density ρ_d that plays a crucial role in determining a spin order. Namely, if $\rho_d=p/q$, where p and q are relative prime numbers, then the period r of a stable phase in one dimension is equal to q or a multiple of q (i.e., $r=nq$, $n=1,2,\ldots$). Consequently, if $r=q$ and q is an odd number, then the system cannot be antiferromagnetic (AF) but ferrimagnetic (FI). Indeed, we observe both FI and AF phases distributed over the whole region between the F and the simplest AF phases. This is in contrast to the results reported in Ref. 18, where many FI phases (named as partially polarized or PP) were missed in one dimension because only systems containing even numbers of lattice sites were taken into account. On the other hand, our AF phases are consistent with NP phases reported in Ref. 18.

It appears that not only the period is determined by ρ_d. We found a remarkable feature concerning the number L_f of changes in the f-electron spin orientation (from up to down or from down to up) calculated per site. If in the diagram displayed in Fig. 1 we move up along a vertical line (i.e., when J is fixed), then L_f of subsequent phases increases with the density ρ_d. What is more, for $J \leq 1$ in almost all cases $L_f=\rho_d$. Then the number of itinerant electrons is equal to the number of pairs of localized electrons with magnetic moments oriented oppositely.

Physically this rule means that each moving electron is somehow associated with an exactly one abrupt change in the potential resulting from the localized electrons. In other words, the minimum energy is attained when the number of moving electrons and the number of changes in the potential acting on them are equal to each other. The rule can be noticed by direct inspection, e.g., looking along the dashed line in Fig. 1 (for $J=0.4$). In this case the unit cells of phases located between F and the simplest AF phases are displayed in Table I.

Obviously, for small enough ρ_d, where the F phase is stable, one has $L_f=0$ and for $\rho_d=1$, where the simplest AF phase is stable, one has $L_f=1$. So it is clear that in one dimension the density of itinerant electrons ρ_d not only determines the periodicity (within an accuracy to a small natural number multiplier) of the arrangement of the f electrons but also strongly influences the relative distribution of spins up and down inside unit cells.

In two dimensions the process of transformation from F to AF with an increase in ρ_d can be divided into two stages (see Fig. 2). First, anisotropic quasi-one-dimensional structures composed of parallel ferromagnetic chains oriented along one of the main lattice axis are formed. We call the area *the region of axial stripes with ferromagnetic chains* (see Figs. 2 and 3). For $J \lesssim 3.05$ this region ends up with the simplest phase belonging to this class, which is composed of ferromagnetic chains with alternating spin directions. In our considerations this is the very special phase, as it can be also viewed as composed of the simplest antiferromagnetic chains along the perpendicular axis. This is why we call the phase AF-f/a, to underline that it is the antiferromagnetic phase composed of ferro-/antiferromagnetic chains (see Figs. 2 and 3).

Above the stability region of AF-f/a, the majority of phases (see Fig. 3) are composed of either only the simplest antiferromagnetic chains (for $J \lesssim 1.2$) or with an admixture of ferromagnetic chains (for $J \gtrsim 1.8$) and in the intermediate interval of $1.2 \lesssim J \lesssim 1.8$ also of ferrimagnetic chains. Some phases found in this region can be viewed as composed of diagonal ferromagnetic chains oriented along the diagonal (1,1) direction. The final stage of the transformation of the phases with an increase in ρ_d is the simplest AF phase with antiferromagnetic chains located along the both main lattice axes.

It appears that the transformation from F to the simplest AF phase is accompanied with an increase in the rate of localization of itinerant electrons, as with an increase in ρ_d the mobility of the d electrons becomes more and more restricted when the half filling is approached. For small ρ_d, where the F phase is stable, the f electrons act on the d electrons as a uniform site-independent external field that does not disturb their movements. Then, in the region of axial stripes with ferromagnetic chains, the d electrons can move easily but only along these chains, as along the perpendicular direction an external potential (coming from the f

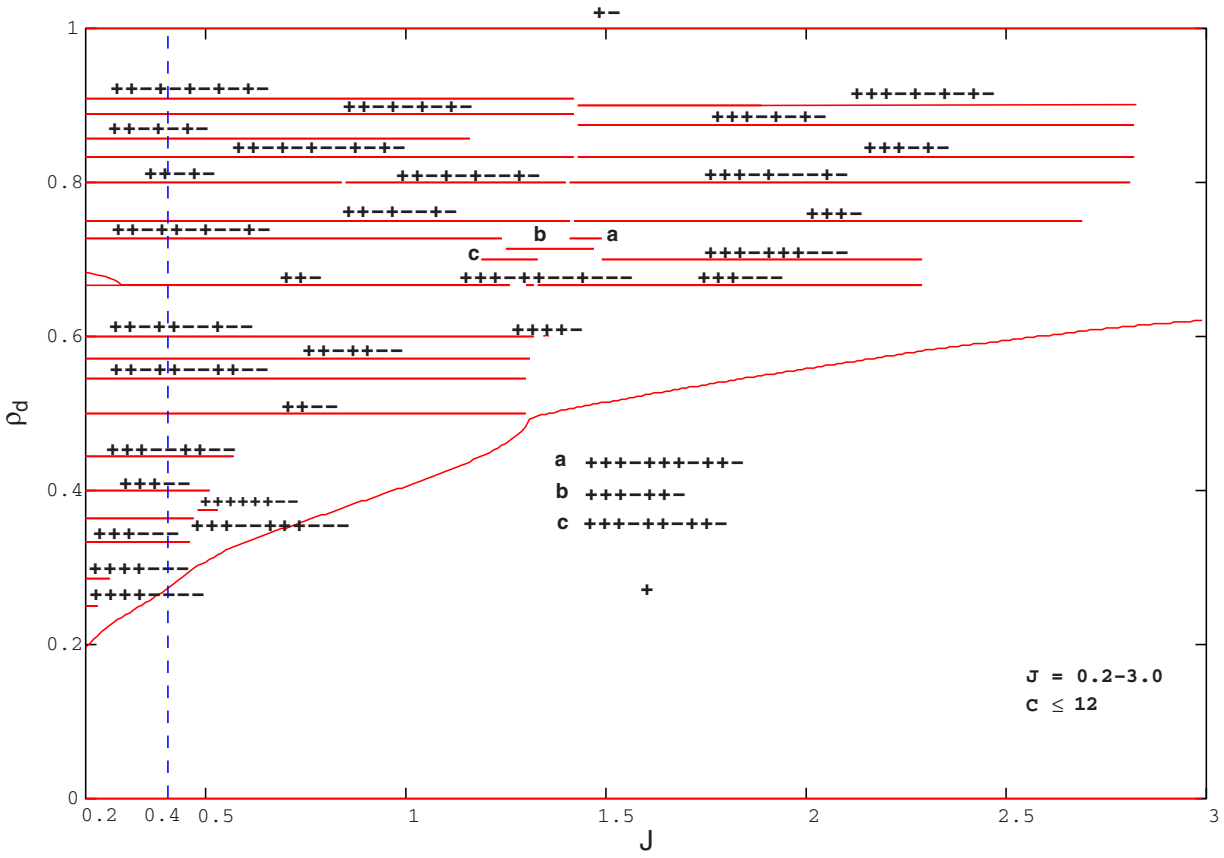

FIG. 1. (Color online) The one-dimensional pure magnetic phase diagram restricted to all periodic phases with $\rho_f=1$ and with the maximum period $C\leq 12$. The straight-line segments mark stability intervals of the phases. Unit cells of the phases are expressed by sequences of the plus and minus signs placed close to (in almost all cases just above) the corresponding line segments. The signs "+" and "−" denote up- and down-spins of the f electrons, respectively. The extended area below the curve line at the bottom of the diagram shows a stability region of the ferromagnetic phase. Unit cells of phases located along the dashed vertical line for $J=0.4$ are displayed in Table I.

electrons) alternates by taking the two different values $U+J$ and $U-J$, which causes scattering of the d electrons.

The AF-f/a phase is an optimal one with respect to the transport of the d electrons through the lattice but only along one direction. Maybe it is related to the optimum doping reported in some materials, when there is a balance between a density of current carriers and their mobility over the lattice. Obviously, one should be cautious when trying to relate the results obtained for such a simple model with situations observed in real materials. However it is interesting that the optimum doping observed here is attained for ρ_d close to 0.5, which corresponds to the special case of quarter filling.

A further increase in ρ_d causes a complete vanishing of ferromagnetic chains for small values of J ($J\lesssim 1.2$) and a gradual decrease in their number for not too small J. It means that the d electrons meet more and more potential barriers in any direction, which makes them more and more localized. Obviously, the rate of localization becomes higher when J is large.

Here we point out another interesting feature of the model. Namely, the critical value ρ_d^* below which phases containing antiferromagnetic chains are stable increases with J, so the range of densities ρ_d where the d electrons become more localized shrinks, but at the same time the rate of the localization becomes more pronounced. It means that for

TABLE I. Unit cells of phases located along the dashed line $J=0.4$ in Fig. 1 and electron densities $\rho_d(=L_f)$ corresponding to them.

Unit cell	ρ_d
++−−−	1/3
++−−++−−−	4/11
++−−−	2/5
++−−++−−	4/9
++−−	1/2
++−−++−−++−−	6/11
++−−++−−	4/7
++−−++−−+−−	3/5
++−	2/3
++−−++−+−−+−	8/11
++−+−−+−	3/4
++−+−	4/5
++−+−+−−+−+−	5/6
++−+−+−	6/7
++−+−+−+−	8/9
++−+−+−+−+−	10/11
+−	1

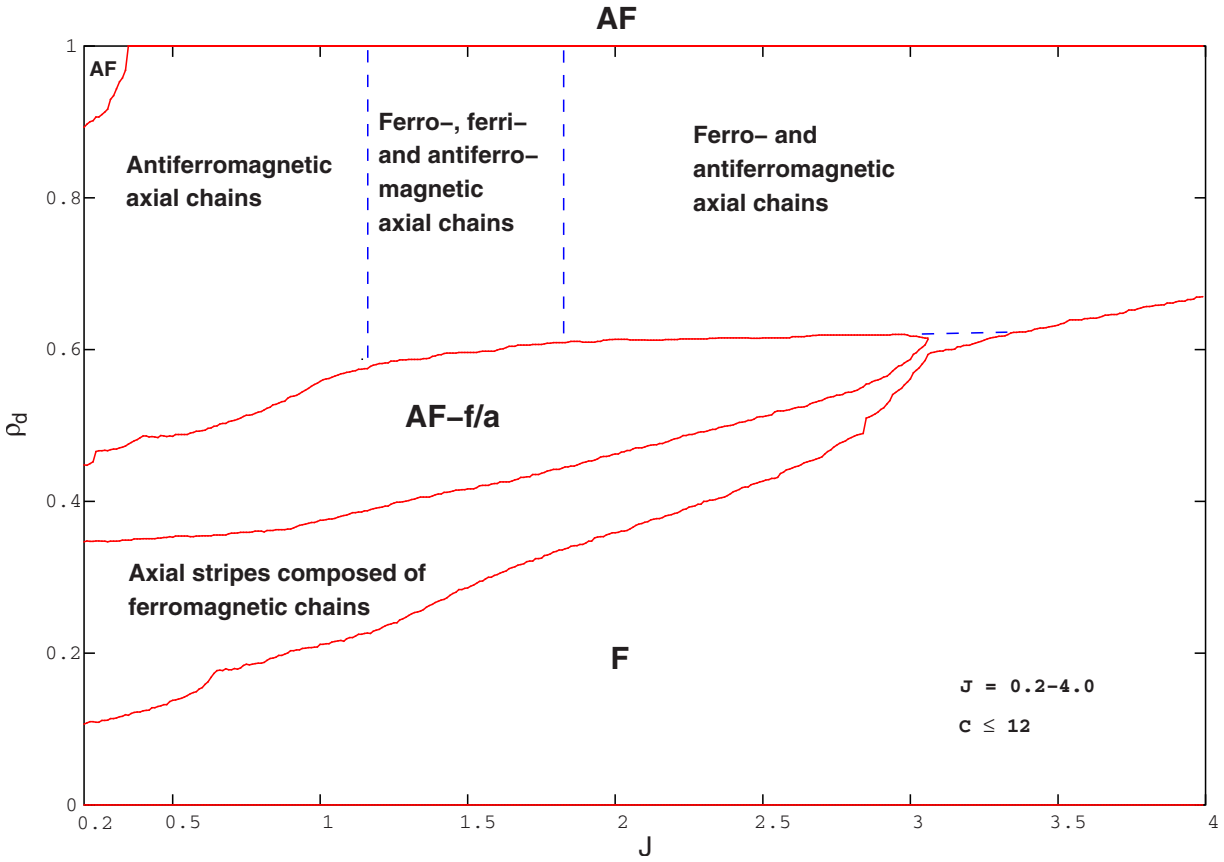

FIG. 2. (Color online) The two-dimensional pure magnetic phase diagram restricted to all periodic phases with $\rho_f=1$ and $C\leq 12$. Typical configurations of the spins of the f electrons representing phases from particular regions of the diagram are shown in Fig. 3.

large J the d electrons pass from a delocalized to a localized regime within a relatively small interval of their densities. Moreover the reported results suggest that in the limit of infinite J, the interval between the conducting F and the insulating AF phases tends to zero (close to the line $\rho_d=1$). This may be regarded as an analogy to the famous Nagaoka problem studied within the Hubbard model.

B. Diluted magnets

Let us now analyze a phase diagram corresponding to a diluted magnet, where both spin and charge orderings are relevant. The diagram is displayed on the (ρ_f,ρ_d) plane for $U=2$ and $J=0.5$ in the 1D case (see Fig. 4) and for $U=4$ and $J=0.5$ in the 2D case (see Fig. 5). The maximum period C of allowed phases in the two cases is equal to 8. The values of the parameters U and J were chosen to be characteristic intermediate value representatives.

We found that in both the 1D and the 2D diagrams the majority of periodic phases are located along one of the following three lines: $\rho_f=1-\rho_d$, $\rho_f=2-\rho_d$, or the diagonal $\rho_f=1-\rho_d/2$. The first two mentioned lines correspond to mixed-valence regimes.

Both antiferro- and ferrimagnetic arrangements of the f electrons are found in the whole range of ρ_f and ρ_d in one dimension and two dimensions. In one dimension the unit cells of phases located along the line $\rho_f=1-\rho_d$ are composed of blocks of spins up (+) and down (−), whereas the pairs of opposite spins (+−) are stable along the $\rho_f=2-\rho_d$ line. The unit cells of phases located along the diagonal $\rho_f=1-\rho_d/2$ have the most homogeneous types of structures. A typical example of the transformation can be noticed, e.g., for $\rho_f=2/3$, where the unit cell $\{oo++--\}$ transforms first to $\{o++o--\}$ and then to $\{o+-\}$ for $\rho_d=1/3$, 2/3, and 4/3, respectively.

In two dimensions (see Figs. 5 and 6), phases located along the $\rho_f=1-\rho_d$ line are composed of ferromagnetic (or diluted ferromagnetic) and nonmagnetic chains oriented along one of the lattice axis (e.g., D1 in Fig. 6). Phases belonging to this family are marked on the diagram in Fig. 5 by straight-line segments. It means that they are stable over finite intervals of band fillings.

On the other hand, phases located along the $\rho_f=2-\rho_d$ line are composed of antiferromagnetic and nonmagnetic chains. Phases located along the diagonal $\rho_f=1-\rho_d/2$ can be viewed as composed of diluted ferro- or antiferromagnetic chains (D2–D4 in Fig. 6). The highest symmetry has the phase D3 placed at the central point of the diagram ($\rho_f=1/2$, $\rho_d=1$).

It is interesting that phases located along the diagonal $\rho_f=1-\rho_d/2$ are insulating for any values of the model parameters we examined, as they have gaps at their Fermi levels, whereas phases found along the line $\rho_f=1-\rho_d$ have no energy gaps at their Fermi levels. Phases located along the line $\rho_f=2-\rho_d$ have no gaps for small values of U, but they do have gaps for large enough U. This is consistent with the

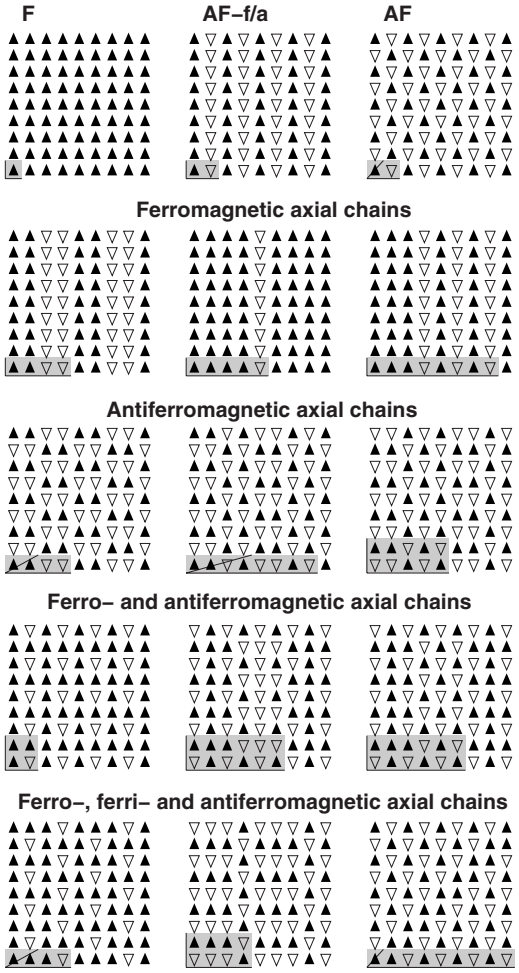

FIG. 3. Examples of ground-state periodic phases found in the diagram displayed in Fig. 2. The symbol ▲ (▽) denotes a spin-up (-down) f electron. The shaded rectangles in the left bottom parts of the pictures mark unit cells of the corresponding phases. The straight-line segments mark the translation vectors.

conjecture that the d electrons can easily (i.e., without scattering) move along ferromagnetic and nonmagnetic chains. However along antiferromagnetic chains their mobility becomes suppressed.

IV. SUMMARY AND DISCUSSION

Since the diagrams reported in this paper were constructed within the restricted space of periodic configurations, they can serve only as skeletons of the full diagrams. Here, similar to what was found in the case of the simplest FKM,[10] most of the diagrams' areas are occupied by mixtures of various phases, occasionally penetrated by periodic phases.

With an increase in the maximum period C of admissible configurations, more and more periodic phases with higher periods replace some of the mixtures on the canonical phase diagrams. However, we observed that the higher period phases do not destroy the diagrams' structure; i.e., the charge and spin distributions of these new phases follow the same rules that we already detected for low period phases. So our conjecture is that the full diagrams will be filled with phases whose charge and magnetic order can be easily predicted (for a given set of the coupling parameters and densities ρ_d and ρ_f). Of course, working within the RPDM, we are not able to prove the statement rigorously. However, since it appears to be quite reasonable, we expect that it can be established definitely by other methods.

In the limiting case of C tending to infinity, not only periodic but also aperiodic phases may happen to appear on the diagrams. It is not clear if some mixtures of low period phases survive in the central region of the full phase diagram. However it is quite possible, as in the simplest spinless FKM such phases are proven to have the lowest energy in the large U limit.[22]

The rules of the formation of the phases we detected from an analysis of the diagrams do not allow determining unambiguously the ground-state charge and spin arrangement for given values of ρ_f, ρ_d, U, and J. However they provide enough information needed for a rough prediction of what sorts of phases appear on the diagrams and where they are located.

In the pure magnetic case ($\rho_f=1$), the F phase is stable for the densities ρ_d such that $\rho_d<\rho_d^*(J)$ or $2-\rho_d^*(J)<\rho_d$, where $\rho_d^*(J)$ is an increasing function of J. Within the interval of J ranging from 0.2 to 3.0, the function $\rho_d^*(J)$ increases from about 0.2 to slightly above 0.6 in one dimension (see Fig. 1) and from about 0.1 to around 0.55 in two dimensions (see Fig. 2). The results are consistent with the data obtained in Ref. 18.

When ρ_d tends to the half filling $\rho_d=1$, a transformation from F to the simplest AF phase occurs in one dimension according to the following simple rules:

(1) If $\rho_d=p/q$, where p and q are relative prime integers, then if a phase is periodic, its period is equal to nq ($n=1,2,\ldots$).

(2) For small J and $\rho_d=p/q$, with q being an even integer, periodic phases are antiferromagnetic, whereas for q that is an odd number they are ferrimagnetic with the lowest possible magnetization. For large J higher magnetizations states become stable.

(3) For a given J the number L_f of changes in spin orientation calculated per site increases with ρ_d and for small J it is equal to ρ_d.

(4) For a given density ρ_d the number L_f drops with an increase in J.

The rules confirm the presence of quite well organized phase diagram structure not revealed in previous studies. In fact, some of the details shown in Ref. 18, such as, for example, arrangements of spins in a certain number of phases, are in agreement with these rules. However, since only rings composed of even numbers of sites and even numbers of electrons were investigated in Ref. 18, a number of FI phases were missed.

The driving mechanisms that are behind the detected rules are still not fully understood. Recently Brydon and Gulácsi[23] discovered that competitive roles of the forward-scattering and backscattering of itinerant electrons can explain the observed richness of the spinless FKM diagrams. We hope that studies carried out along similar ways could be also performed for the extended version of the FKM with the Hund

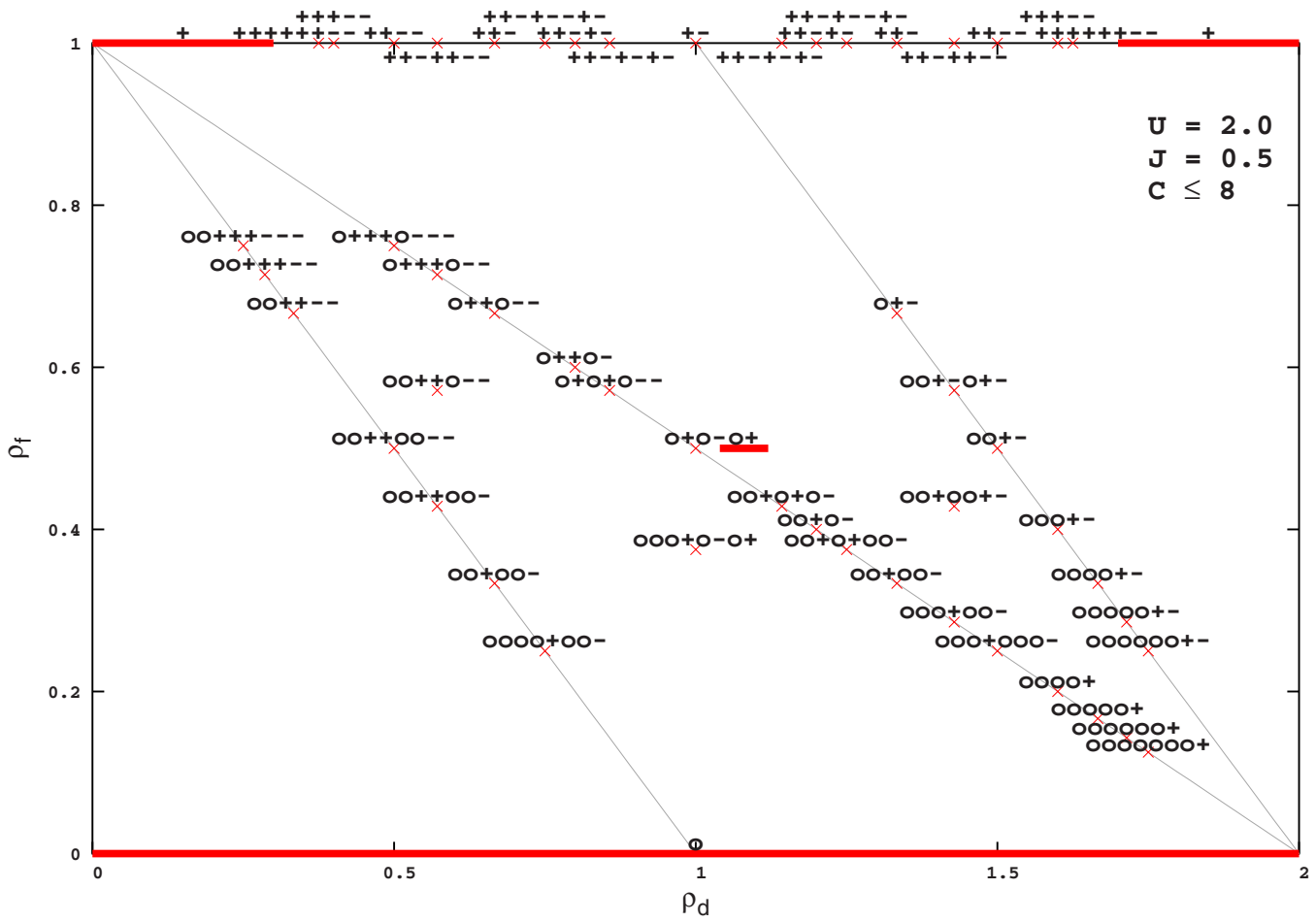

FIG. 4. (Color online) The canonical phase diagram of the extended FKM with Hund coupling for the 1D lattice and $U=2$, $J=0.5$. The crosses $\times$ and horizontal straight-line segments mark stability points or intervals of periodic phases. Their unit cells are drawn as sequences of small circles and plus and minus signs, which correspond to sites nonoccupied and occupied by the spin-up and occupied by the spin-down f electrons, respectively.

coupling and elucidate the rules we observed.

In two dimensions the situation is more complex and we were not able to find out as many precise rules as in the 1D case, even though our phase diagram shows more regularities than those reported in Ref. 18. First of all, we noticed that all phases that appear in the diagram are composed of ferromagnetic or antiferromagnetic chains. For intermediate values of J they are also composed of ferrimagnetic chains parallel to each other. Obviously, the phases with only ferromagnetic chains have one-dimensional unit cells and they form axial stripes. These phases occur within an interval of electron densities ρ_d neighboring to those for which the F phase is stable. For $J \lesssim 3.05$ the interval ends with the simplest phase belonging to the family, the AF-f/a phase (see Fig. 2), which separates regions of axial stripes from those of containing antiferromagnetic chains. (Ferromagnetic and ferrimagnetic chains could be also present for not too small values of J.) So for ρ_d out of the stability regions of F, AF-f/a, and axial stripes, almost all phases are composed of either exclusively antiferromagnetic chains or with an admixture of ferri- and ferromagnetic chains. Some of them containing only ferro- and antiferromagnetic chains are ferrimagnetic.

An analysis of diluted magnets diagrams (see Figs. 4–6) also permits us to fix some rules of charge and spin formation and its evolution with a change in the densities ρ_d and ρ_f. Here we focused on the most representative three families of the phases. One of them consists of phases located along the main diagonal. This family corresponds to the most homogeneous phases relevant for the spinless FKM. This is the only family of diluted periodic phases which is left in the limit of large U (if we keep J considerable smaller than U). Phases belonging to this family are characterized by the most uniform charge distribution but not necessarily the most uniform magnetic distribution. In two dimensions all but one particular phase have a form of sloped stripes composed of parallel lines of ferromagnetic chains (see configurations D2 and D4 in Fig. 6). The only exception is the most symmetric antiferromagnetic chessboard phase D3 placed in the center of the diagram. The phase has two-dimensional unit cell of size 2×2 and is composed of diluted ferromagnetic lines (see Fig. 6).

Two other characteristic families refer to mixed-valence regimes, for which either of the conditions $\rho_d+\rho_f=1$ or $\rho_d+\rho_f=2$ is fulfilled. These phases are ground states only for small and intermediate values of U (and $U \gg J$). In one dimension, it appears that unit cells of phases belonging the first category ($\rho_d+\rho_f=1$) are built of blocks of spins up separated by pairs of empty sites from blocks of spins down. On

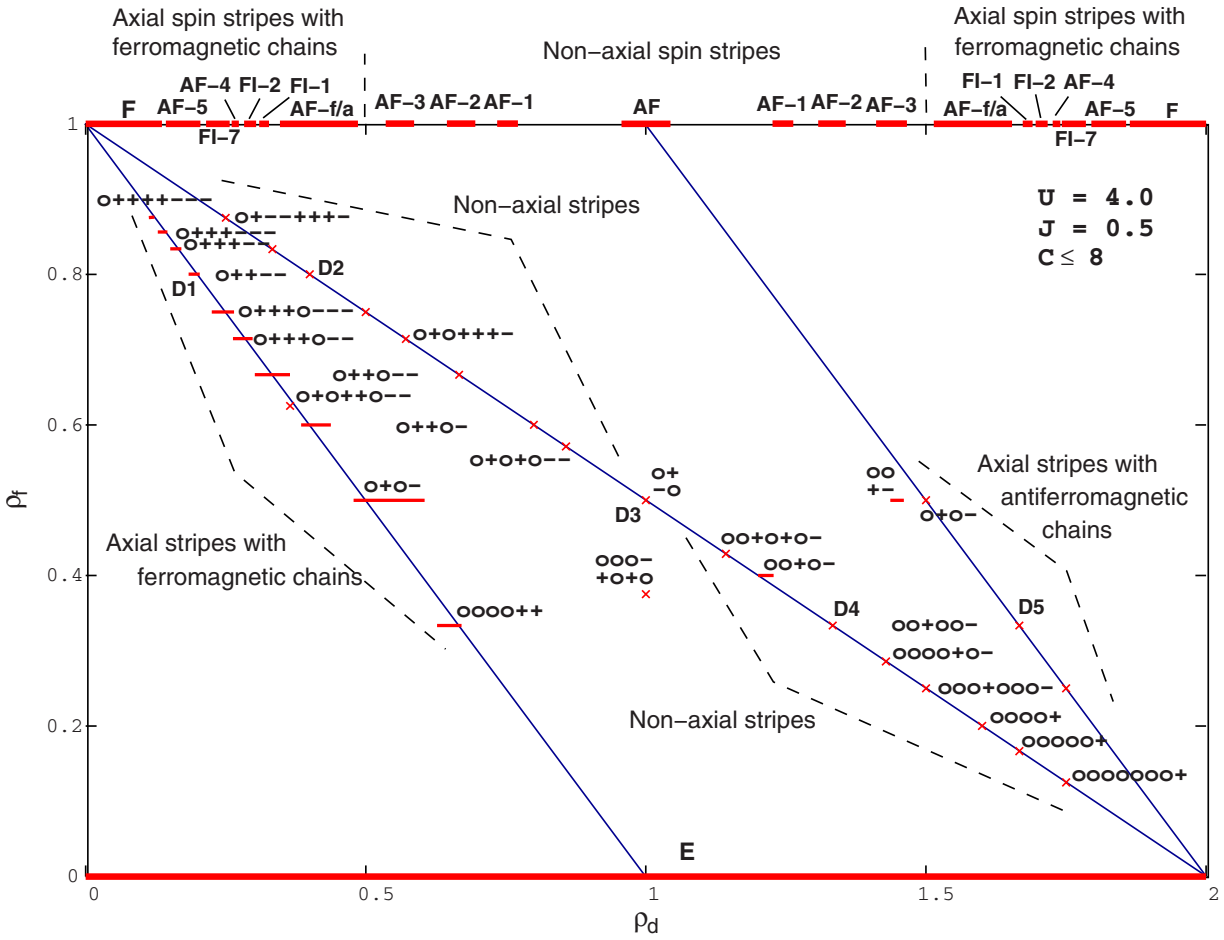

FIG. 5. (Color online) The canonical phase diagram of the extended FKM with Hund coupling for the 2D square lattice and $U=4$, $J=0.5$. The lines $\rho_f=1-\rho_d$, $\rho_f=2-\rho_d$, and $\rho_f=1-\rho_d/2$ are merely visual guides. The crosses $\times$ and horizontal straight-line segments mark stability points and intervals of the periodic phases, respectively. Their unit cells are drawn as sequences of small circles and plus and minus signs, which correspond to sites nonoccupied and occupied by the spin-up and occupied by the spin-down f electrons, respectively. A number of pairs of phases have the same unit cells but different translation vectors. Unit cells of the phases are displayed along the horizontal lines in the middle between the lines $\rho_f=1-\rho_d$ and $\rho_f=1-\rho_d/2$ and in the middle between the lines $\rho_f=1-\rho_d/2$ and $\rho_f=2-\rho_d$. The configurations located along the line $\rho_f=1$ are presented in Fig. 3. A set of characteristic configurations D1–D5 is shown in Fig. 6.

the other hand, unit cells of phases belonging to the second category ($\rho_d+\rho_f=2$) consist of empty sites separated by pairs of oppositely oriented spins (+−).

In two dimensions, all phases coming from the both mixed-valence categories have the form of axial stripes. So they have the same type of charge ordering. Nevertheless their magnetic orders are clearly different, as phases that belong to the first class are composed of ferromagnetic chains (e.g., D1 in Fig. 6), whereas phases for which the condition $\rho_d+\rho_f=2$ is fulfilled are composed of antiferromagnetic chains (e.g., D5 in Fig. 6).

Our current studies confirm findings reported in Ref. 6 that show that the compromise between kinetic energy of the d electrons and their interaction with the f electrons imposes the formation of superstructures with shapes of stripes. Kinetic energy tends to spread out the d electrons uniformly over the lattice. However due to the presence of localized magnetic ions, a kind of d-electron density deformation must occur. Obviously, the deformation has to be conjugated with an arrangement of the f electrons. Apparently, the simplest departures from the homogeneity that are preferred have the form of axial or diagonal stripes.

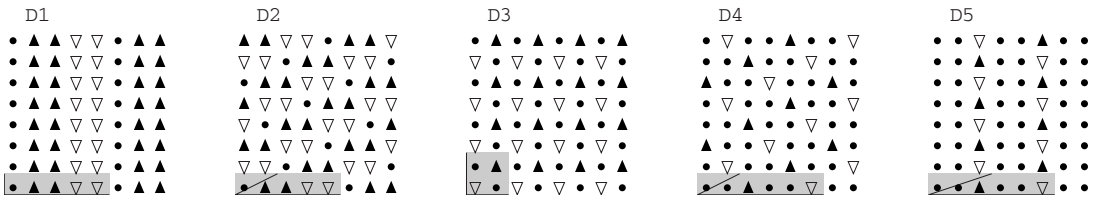

FIG. 6. Characteristic ground-state configurations displayed in Fig. 5. See the caption to Fig. 3 for more explanations.

Perhaps the most important conclusion emerging from this work is that the observed rules of the formation of the phases suggest the possibility of manipulation of positional arrangements of magnetic ions diluted in the system and also their magnetic alignment with a change in doping. For example, one should be able to tune a modulation of charge and/or spin (stripes' width). If it can be done in a controllable way, then in systems that can be described by the model, it would be possible to change gradually the orientation of stripe phases (between axial and diagonal) and to change the magnetic order along chains (from ferromagnetic through ferrimagnetic up to antiferromagnetic).

We hope that the results will motivate some new experimental work focusing on searching relationships between density of current carriers (electrons or holes) and observed charge and/or magnetic superstructure. According to our findings complicated ordering patterns should emerge from on-site interactions of localized and moving electrons and a simplified version of Hund's rule. Therefore, we expect that experimental realizations of such patterns are robust in those correlated electron systems where a substantial anisotropy of spin-spin interactions occur.

ACKNOWLEDGMENTS

We thank J. K. Freericks, M. Maśka, and J. Jędrzejewski for valuable comments and critical reading of the paper.

[1] R. Kajimoto, K. Ishizaka, H. Yoshizawa, and Y. Tokura, Phys. Rev. B **67**, 014511 (2003).

[2] V. J. Emery, S. A. Kivelson, and H. Q. Lin, Phys. Rev. Lett. **64**, 475 (1990); E. W. Carlson, S. A. Kivelson, Z. Nussinov, and V. J. Emery, Phys. Rev. B **57**, 14704 (1998); L. P. Pryadko, S. A. Kivelson, and D. W. Hone, Phys. Rev. Lett. **80**, 5651 (1998); L. P. Pryadko, S. A. Kivelson, V. J. Emery, Y. B. Bazaliy, and E. A. Demler, Phys. Rev. B **60**, 7541 (1999).

[3] S. R. White and D. J. Scalapino, Phys. Rev. Lett. **80**, 1272 (1998); **81**, 3227 (1998); Phys. Rev. B **60**, R753 (1999); **61**, 6320 (2000).

[4] W. O. Putikka, M. U. Luchini, and T. M. Rice, Phys. Rev. Lett. **68**, 538 (1992); W. O. Putikka and M. U. Luchini, Phys. Rev. B **62**, 1684 (2000).

[5] A. C. Cosentini, M. Capone, L. Guidoni, and G. B. Bachelet, Phys. Rev. B **58**, R14685 (1998); M. Calandra, F. Becca, and S. Sorella, Phys. Rev. Lett. **81**, 5185 (1998); C. S. Hellberg and E. Manousakis, Phys. Rev. B **61**, 11787 (2000).

[6] J. Zaanen and A. M. Oleś, Ann. Phys. **5**, 224 (1996); D. Góra, K. Rościszewski, and A. M. Oleś, Phys. Rev. B **60**, 7429 (1999); M. Raczkowski, R. Frésard, and A. M. Oleś, *ibid.* **73**, 174525 (2006); **73**, 094429 (2006).

[7] A. O. Sboychakov, K. I. Kugel, and A. L. Rakhmanov, Phys. Rev. B **76**, 195113 (2007); K. I. Kugel, A. L. Rakhmanov, and A. O. Sboychakov, Physica B (Amsterdam) **403**, 1616 (2008).

[8] E. Dagotto, Rev. Mod. Phys. **66**, 763 (1994); C. S. Hellberg and E. Manousakis, Phys. Rev. Lett. **83**, 132 (1999).

[9] P. Wróbel, Phys. Rev. B **74**, 014507 (2006); P. Wróbel, A. Maciąg, and R. Eder, J. Phys.: Condens. Matter **18**, 1249 (2006).

[10] R. Lemański, J. K. Freericks, and G. Banach, Phys. Rev. Lett. **89**, 196403 (2002); J. Stat. Phys. **116**, 699 (2004).

[11] V. Derzhko and J. Jędrzejewski, Physica A **349**, 511 (2005); J. Stat. Phys. **126**, 467 (2007); V. Derzhko, J. Phys. A **39**, 11145 (2006).

[12] R. Lemański, Phys. Rev. B **71**, 035107 (2005); Phys. Status Solidi B **242**, 409 (2005); **243**, 347 (2006); J. Magn. Magn. Mater. **310**, e327 (2007).

[13] K. Held and D. Vollhardt, Eur. Phys. J. B **5**, 473 (1998).

[14] D. J. Garcia, K. Hallberg, B. Alascio, and M. Avignon, Phys. Rev. Lett. **93**, 177204 (2004).

[15] Th. Pruschke and R. Bulla, Eur. Phys. J. B **44**, 217 (2005).

[16] J. Fröhlich and D. Ueltschi, J. Stat. Phys. **118**, 973 (2005).

[17] D. J. Garcia, K. Hallberg, C. D. Batista, M. Avignon, and B. Alascio, Phys. Rev. Lett. **85**, 3720 (2000); H. Aliaga, B. Normand, K. Hallberg, M. Avignon, and B. Alascio, Phys. Rev. B **64**, 024422 (2001).

[18] P. Farkašovký and H. Čenčariková, Eur. Phys. J. B **47**, 517 (2005).

[19] J. Lach, R. Łyżwa, and J. Jędrzejewski, Phys. Rev. B **48**, 10783 (1993); Z. Gajek, J. Jędrzejewski, and R. Lemański, Physica A **223**, 175 (1996).

[20] G. I. Watson and R. Lemański, J. Phys.: Condens. Matter **7**, 9521 (1995).

[21] Only these kinds of phases were taken into account in our previous papers where the model was considered.

[22] T. Kennedy, J. Stat. Phys. **91**, 829 (1998).

[23] P. M. R. Brydon and M. Gulácsi, Phys. Rev. B **73**, 235120 (2006).